



## Layer-by-Layer Assembly of Graphene and Au@Pt Nanostructures and Its Application in Catalytic Oxidation of Methanol

JIANFENG FAN<sup>1,2,\*</sup>, YINGJIN WANG<sup>1</sup>, LIQING LI<sup>2</sup>, LINA GAO<sup>2</sup> and LOUZHEN FAN<sup>2</sup>

<sup>1</sup>Department of Chemistry, Xinzhou Teachers' University, Xinzhou 034000, Shanxi Province, P.R. China

<sup>2</sup>Department of Chemistry, Beijing Normal University, Beijing 100875, P.R. China

\*Corresponding author: E-mail: [fjf3034832@126.com](mailto:fjf3034832@126.com)

Received: 7 September 2013;

Accepted: 31 December 2013;

Published online: 28 July 2014;

AJC-15629

Layer-by-layer films comprised of alternating graphene and Au@Pt nanostructures layers are readily produced by the three-step procedure involving the preparation of Au colloid, Au nanoparticles entering the layers of graphite, followed by Au@Pt nanostructures' formation by electrochemical methods on the graphene nanosheet. X-ray diffraction and Raman scattering showed the Au@Pt nanostructures/graphene was fabricated. Electrocatalytic properties of the resulting Au@Pt nanostructures/graphene electrode for methanol oxidation reaction were investigated. Compared with Au@Pt nanostructures/graphite, an appreciably improved electronic conductivity was observed for the Au@Pt nanostructures/graphene electrode.

**Keywords:** Graphene, Au@Pt nanostructures, Assembly, Catalytic oxidation.

### INTRODUCTION

Graphene as a new branch of carbon materials, numerous research efforts are underway directed at discovering the superior and unique properties of single layer graphene and multilayer graphene nanoplatelets<sup>1,2</sup>. Recently, increasing attention has been paid to its serving as the support due to its high surface area, excellent electronic properties and special chemical stability. In particular, graphene-metal nanoparticles hybrid systems have the potential to be very useful in various engineering applications such as fuel cell catalysis<sup>3-7</sup>, electrochemical sensing<sup>8,9</sup> and electrochemical energy storage<sup>10,11</sup>.

Nano-sized Pt particles are the most commonly used anode electrocatalysts in direct methanol fuel cells. The Pt/graphene hybrids were obtained mainly *via* reducing Pt ions and graphene oxide simultaneously<sup>12</sup>. However, these methods involve highly toxic chemicals, such as hydrazine hydrate, high temperature and multiple steps that are time or labor consuming<sup>13</sup>. More notably, the resulting graphene sheets are not separated by Pt nanoparticles since these Pt nanoparticles are mostly located on the surface of graphene films. Furthermore, for pure Pt, the activity towards methanol oxidation is hindered by CO poisoning. Consequently, Pt-based alloy or core-shell nanoelectrocatalysts were developed to improve both the electrocatalytic activity and stability of the electrocatalysts. Therefore, deposited Pt core-shell nanoparticles on graphene nanosheet, giving rise to significant modification to the properties of Pt

nanoparticles electrocatalysts and high activities for methanol oxidation reaction was observed. This indicates that graphene could be a superb catalyst support for fuel cells<sup>12</sup>. However, the uneven size and bad dispersivity of the obtained Pt core-shell nanoparticles and the defects of graphene oxide were all unfavorable to the electrocatalytic activity of the hybrid. Thus, a simple method for fabricating high-performance Pt core-shell nanoparticles/graphene hybrid has aroused wide attention.

Little information has been reported on the layer-by-layer films comprised of alternating graphene and Au@Pt nanostructures layers. In this work, a modified three-step seed-mediated growth method was used for synthesizing Au@Pt/graphene hybrid. Gold colloid, comprising of Au nanoparticles of about 10 nm in diameter, was synthesized as seeds (cores). Subsequently, it was mixed with the expanded graphite where the Au nanoparticles intercalated and adhered to the layers of graphene sheets during the sonication process. Finally, the uniform Au@Pt nanostructures were overgrown on the Au cores with high yield on the surface of graphene sheets by electrochemical method. Layer-by-layer assembly of graphene and Au@Pt nanostructures was fabricated. It is important to note that the graphene sheets were directly exfoliated from the expanded graphite with small defects in this approach, which can improve its performance. Moreover, methanol oxidation reaction catalyzed by Au@Pt/graphene and Au@Pt/graphite catalysts was investigated respectively; the Au@Pt/graphene catalyst showed better catalytic effect onto this reaction.

## EXPERIMENTAL

Potassium tetrachloroplatinate (II) ( $K_2PtCl_4$ , 99.9 %-Pt, Newburyport, USA), potassium hexachloroplatinate (IV) ( $K_2PtCl_6$ , 40 % Pt, New Jersey, USA), hydrogen tetrachloroaurate (III) hydrate ( $HAuCl_4$ , Aldrich), Natural graphite (spectrum pure, about 50  $\mu m$ , Shanghai Carbon Co. Ltd.). Sodium citrate, *N,N*-dimethylformamide (DMF), sulfuric acid ( $H_2SO_4$ ) and methanol ( $CH_3OH$ ) were purchased from Beijing Chemical Factory (China). All chemicals were analytical grade in addition to graphite and used without further purification. Distilled water was used in all experiments.

**Characterization:** The morphologies and energy dispersive X-ray (EDX) of samples on the ITO substrates were directly subjected to characterize with a Hitachi S4800 scanning electron microscope (SEM). For the high-resolution transmission electron microscope (HRTEM, Tecnai F20) measurements, the samples were scraped from the ITO substrates into ethanol and then cast onto the copper grids by placing a drop of solution. Power X-ray diffraction (XRD) measurements were performed on a X' Pert PRO MPD (PAN alytical B.V.) using  $CuK_{\alpha}$  radiation of 40 kV and 40 mA. The resonant Raman spectra were recorded on a Lab RAM Aramis Smart Raman Spectrometer (Horiba Jobin Yvon company) with a 632.8 nm line of a He-Ne laser as the excitation sources. Cyclic voltammetry (CV) studies were performed by using a CHI705 electrochemical workstation (CH Instruments, Inc. USA) with a conventional three-electrode electrochemical cell in which the Au@Pt nanostructures/graphene nanosheet hybrid (which have been prepared by electrochemical deposition) on the ITO substrate were used as the working electrode, a platinum wire was used as the counter and a SCE was used as the reference.

### Preparation

**Synthesis of Au colloid:** A 10 mL portion of sodium citrate solution (3.4 mM) was heated to boiling. While stirring vigorously, 1 mL  $HAuCl_4$  aqueous solution (8.7 mM) was added rapidly. The solution was maintained at the boiling point for 1 h. The heating source was removed and the colloid was cooled to room temperature.

**Preparation of expanded graphite:** Expanded graphite was synthesized from spectral graphite by the modified hummers method. Concentrated  $HNO_3$  (40 mL) was added into a 250 mL flask filled with graphite (2 g), followed by slow addition of  $K_2Cr_2O_7$  (0.28 g). The mixture was stirred at room temperature for 45 min then it was cooled to room temperature and washed with distilled water for several times to adjust the pH to 5-7. Successively, the black powder was isolated *via* centrifugation, washed with distilled water and dried in a vacuum oven at 50  $^{\circ}C$  for 1.5-2 h. After that, the black powder was put into a muffle furnace using a hot plate, heated at 800  $^{\circ}C$  for 1 min, then took out and cooled at room temperature. Finally, the expanded graphite was prepared.

**Preparation of Au nanoparticles/graphene and Au@Pt nanostructures/graphene nanosheet hybrid:** To obtain the Au nanoparticles/graphene, 0.1 mg expanded graphite produced as described above was dispersed in mixture solution of 1 mL Au colloid and 1.5 mL DMF by ultrasonication (KQ-100DE ultrasonic bath, Shanghai Kunshan Ultrasonic

Instrument Co., Kunshan, China, 90 W) for 0.5 h. Au nanoparticles intercalated the layers of expanded graphite flakes, whose layers distance became wide under the effect of DMF and ultrasonication, then the Au nanoparticles adhered to the surface of graphene sheets.

The tin-doped indium oxide on glass (ITO; Shenzhen Hivac Vacuum Photoelectronics Co., Ltd.) was cleaned ultrasonically and sequentially in distilled water, acetone and ethanol for 0.5 h and then 20  $\mu L$  of the resulting mixture was directly cast on ITO electrode surface and evaporated in the solvent at room temperature to prepare the Au nanoparticles/graphene film modified electrode. A clean platinum wire and a saturated calomel electrode (SCE) were used as counter and reference electrodes, respectively, in a three-electrode cell. The Au@Pt nanospheres/graphene was generated by using an amperometric *i-t* curve technique with a potential at -0.3 V in 5 mM  $K_2PtCl_4$  aqueous solution for 60 s and the Au@Pt nanoflowers/graphene was generated in mixture solution of 2 mM  $K_2PtCl_6$  and 1 M  $H_2SO_4$  at 200 s.

**Preparation of Au@Pt nanoflowers/graphite hybrid:** 0.1 mg graphite was dispersed in 2 mL ethanol solution by ultrasonication for 10 min. Then 20  $\mu L$  of the resulting mixture was directly cast on the ITO electrode surface and evaporated the solvent at room temperature. Then 20  $\mu L$  Au colloid was directly cast on electrode surface to prepare the Au nanoparticles/graphite film modified electrode. Then, the synthesis of Au@Pt nanoflowers/graphite hybrid was carried out in the same conditions to prepare Au@Pt nanostructures/graphene.

## RESULTS AND DISCUSSION

Fig. 1 shows that the overall morphology and composition of the sample. Nanospheres and nanoflowers are randomly dispersed on the graphene background, which is due to the presence of Au@Pt nanoparticles. The bright Au@Pt nanoparticles are located above the graphene layer, while the darker ones are under the layer. As illustrated in Fig. 1a, the surface of graphene is densely decorated with Au@Pt nanoparticles. The majority of the core-shell particles adopted sphere shape with mean size of 100 nm. The particles tending to assemble on graphene substrate indicates the highly monodispersed particles size. Au@Pt nanospheres intercalating between graphene sheets prevented graphene agglomeration and made them clearly stratified (Fig. 1b).

To investigate the performance, we further synthesized another kind of core-shell nanoparticles, Au@Pt nanoflowers (Fig. 1d, 1e and 1f) under the similar reaction conditions. The low-magnification SEM image of the as-prepared sample is displayed in Fig. 1d, showing that the obtained product consists of large-scale layer-by-layer assembly structure of graphene and Au@Pt nanoflowers, in which Au@Pt nanoflowers exhibit monodispersed, uniform and flower-like shape with mean size of 100 nm. This is evidenced further by the high-magnification SEM image (Fig. 1e); both sides of the graphene are covered by the Au@Pt nanoflowers that the bright and dark particles are located above and under the graphene layer, respectively. From the energy dispersive X-ray spectroscopy (EDX) of the two samples (Fig. 1c and 1f), it can be seen that Pt, Au and C are the major elements.

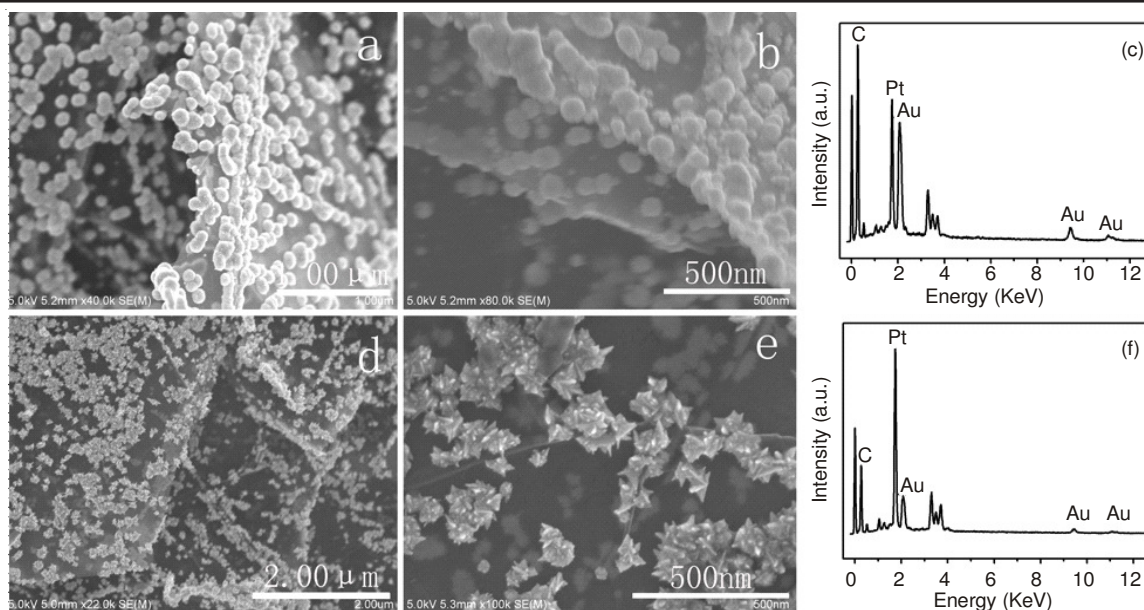


Fig. 1. SEM images of Au@Pt nanostructures/graphene deposited on the ITO substrate: (a) low and (b) high magnification of the Au@Pt nanospheres/graphene nanosheet hybrid, (c) EDX spectrum of Au@Pt nanospheres/graphene, (d) low and (e) high magnification SEM images of Au@Pt nanoflowers/graphene nanosheet hybrid, (f) EDX spectrum of Au@Pt nanoflowers/graphene

Transmission electron micrograph Au@Pt nanoflowers/graphene composite is shown in Fig. 2, there is a clear layered structure of the graphene-metal composite; the Au@Pt nanoflowers sandwich between the transparent graphene layers and the light transmittance of the graphene layer is high. This is consistent with the SEM graphs. It shows that Au@Pt nanoflowers are successfully embedded into the graphene sheets, suggesting strong interactions between the Au@Pt nanoflowers and the graphene sheets.

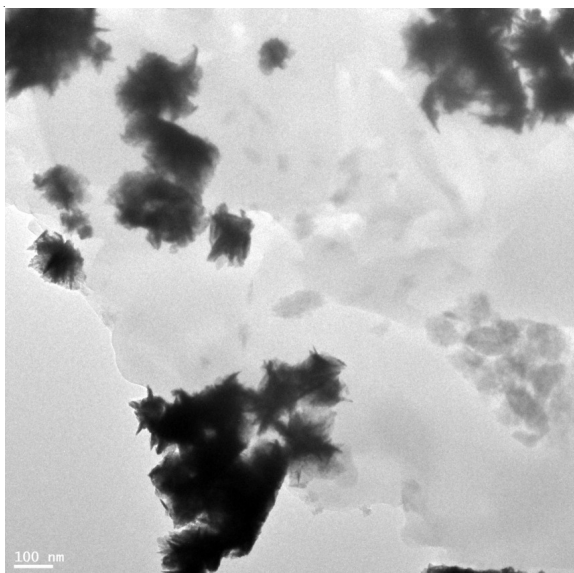


Fig. 2. TEM images of Au@Pt nanoflowers/graphene nanosheet hybrid

The X-ray diffraction pattern of the Au@Pt/graphene nanosheet hybrid is displayed in Fig. 3. The broad peak centered at  $2\theta = 22.70^\circ$  confirmed a random packing of graphene sheets<sup>14</sup>. The stronger intensity at  $2\theta = 81.47^\circ$  can be indexed to the (222) plane of Au. Additionally,  $2\theta = 39.85^\circ$ ,  $46.20^\circ$  and  $67.52^\circ$  can be assigned to (111), (200) and (220)

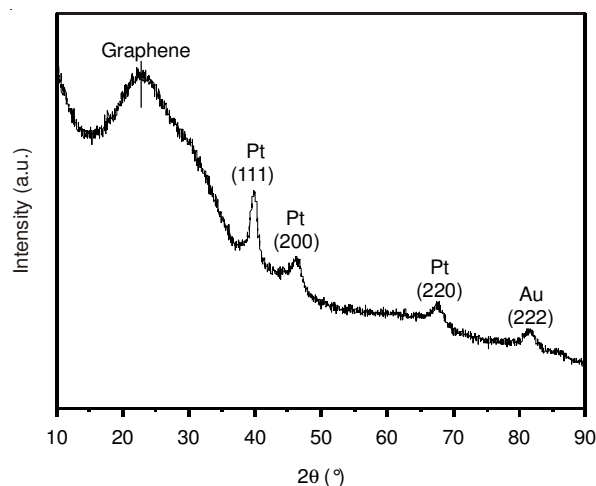


Fig. 3. XRD patterns for Au@Pt/graphene

planes of Pt shells, respectively. There were two distinct phases for Au cores and Pt shells in nanoparticles, indicating that the Au cores do not affect the lattice of the epitaxial grown shell.

The structure of Au@Pt/graphene was examined by Raman spectroscopy (Fig. 4). A weak band at  $1350\text{ cm}^{-1}$  and a strong intensity of band at  $1580\text{ cm}^{-1}$  were assigned to D and G band at graphene layer. The G peak corresponding to the  $E_{2g}$  phonon at the Brillouin zone center and is due to bond stretching of  $sp^2$  carbon pairs in rings and chains. The D peak is due to the breathing modes of six-atom rings and requires a defect for its activation<sup>15,16</sup>. The overtone of the D peak, called 2D peak appears at  $2680\text{ cm}^{-1}$ . Specifically, the 2D peak is distinct, pointed and symmetrical, which can be concluded that the resulting product is graphene.

The catalytic activity of Au@Pt nanostructures/graphene was also evaluated by the electrocatalytic oxidation reaction of methanol, which is expected to be a useful application in the direct methanol fuel cell. Fig. 5 shows typical cyclic voltammetry of Au@Pt nanoflowers/graphene electrode (curve a),

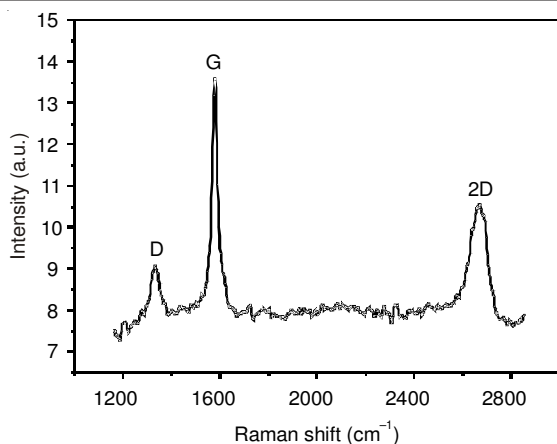


Fig. 4. Raman spectrum for Au@Pt/graphene

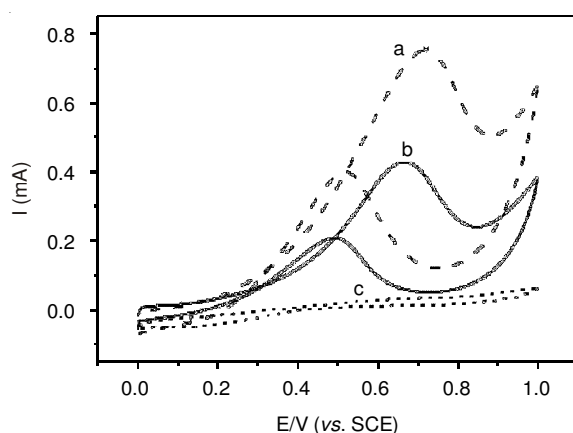


Fig. 5. Cyclic voltammograms of Au@Pt nanoflowers/graphene (a), Au@Pt nanospheres/graphene (b) Au@Pt nanoflowers/graphite (c) electrodes in 2M CH<sub>3</sub>OH + 0.1M H<sub>2</sub>SO<sub>4</sub> solution at room temperature. (scan rate: 100 mV s<sup>-1</sup>)

Au@Pt nanospheres/graphene electrode (curve b) and Au@Pt nanoflowers/graphite electrode (curve c) in 2 M CH<sub>3</sub>OH + 0.1 M H<sub>2</sub>SO<sub>4</sub> solution at room temperature. It is to be noticed that the deposition charges for preparation Au@Pt nanoflowers/graphene, Au@Pt nanospheres/graphene and Au@Pt nanoflowers/graphite electrodes are the same. Assuming the faradaic efficiency for the deposition process is 100 %, the amount of metal Pt in the used three electrodes is same during the catalytic measurement. Notably, the shapes of the cyclic voltammetric curves and peak potentials are in agreement with researches stated elsewhere typically with those using Pt electrode, but the onset potential of methanol oxidation for Au@Pt nanoflowers/graphene electrode occurs at an anodic potential 0.26 V, which is about 50 mV lower than that for Au@Pt nanoflowers/graphite (0.31 V). In addition, the current with the Au@Pt nanostructures/graphene electrode is also higher as compared with the Au@Pt nanoflowers/graphite electrode, which is caused by the layer-by-layer structure of as-prepared Au@Pt nanostructures/graphene in which the Au nanoparticles intercalating between graphene sheets prevented graphene agglomeration and improved the conductivity of the graphene sheets. On the other hand, the ratio of the forward anodic peak current ( $I_f$ ) to the reverse anodic peak current ( $I_b$ ) can be used to describe the catalyst tolerance to carbonaceous species

accumulation. Ordinarily,  $I_f/I_b$  can be used as a performance index of a catalyst for the conversion and a higher  $I_f/I_b$  value implies better oxidation of methanol to CO<sub>2</sub><sup>17</sup>. In our study, the ratio was approximately 2 for the Au@Pt nanoflowers/graphene electrode and 1.8 for the Au@Pt nanospheres/graphene electrode, even higher than the value of 1.4 for the Au@Pt nanoflowers/graphite electrode. Such a high value for Au@Pt nanostructures/graphene electrode indicates that most of the intermediate carbonaceous species were oxidized to CO<sub>2</sub> in the forward scan. This suggests that the interaction of Au@Pt and graphene leads to the less poisoning of Pt by the CO-like intermediates formed during methanol activation. Graphene modified with Au@Pt nanocomposites greatly improved the performance of Pt nanoparticles in methanol electrocatalytic oxidation. Compared to Pt, graphene has a higher work function. When it is combined with Au@Pt nanocomposites, the electrons in the conduction band of Pt can transfer to graphene.

### Conclusion

In conclusion, a convenient and effective three-step seed-mediated growth method for synthesizing Au@Pt/graphene has been successfully conducted. The as-prepared Au@Pt/graphene nanosheet hybrid exhibit significantly higher electrocatalytic activity for the electrocatalytic oxidation of methanol than that of Au@Pt/graphite with similar atomic ratio. The higher electrochemical catalytic activities of Au@Pt/graphene electrodes have been attributed to excellent electronic conductivity properties in the layer-by-layer structures. The successful preparation of Au@Pt nanostructures/graphene nanocomposites opens a new path for an efficient dispersion of the promising electrocatalysts in the direct methanol fuel cells.

### ACKNOWLEDGEMENTS

This work is supported by NNSF of China (21073018) and Scientific and Technological Innovation Programs of Higher Education Institutions in Shanxi (20121023).

### REFERENCES

- J.L. Xiang and L.T. Drzal, *Appl. Mater. Interfaces*, **3**, 1325 (2011).
- M.J. Allen, V.C. Tung and R.B. Kaner, *Chem. Rev.*, **110**, 132 (2010).
- C. Xu, X. Wang and J.W. Zhu, *J. Phys. Chem. C*, **112**, 19841 (2008).
- E. Yoo, T. Okata, T. Akita, M. Kohyama, J. Nakamura and I. Honma, *Nano Lett.*, **9**, 2255 (2009).
- Y.M. Li, L.H. Tang and J.H. Li, *Electrochem. Commun.*, **11**, 846 (2009).
- B. Seger and P.V. Kamat, *J. Phys. Chem. C*, **113**, 7990 (2009).
- C.Z. Zhu, S.J. Guo, Y.M. Zhai and S.J. Dong, *Langmuir*, **26**, 7614 (2010).
- J. Lu, I. Do, L.T. Drzal, R.M. Worden and I. Lee, *ACS Nano*, **2**, 1825 (2008).
- S.J. Guo, D. Wen, Y.M. Zhai, S.J. Dong and E. Wang, *ACS Nano*, **4**, 3959 (2010).
- Y.C. Si and E.T. Samulski, *Chem. Mater.*, **20**, 6792 (2008).
- Y.M. Li, X.J. Lv, J. Lu and J.H. Li, *J. Phys. Chem. C*, **114**, 21770 (2010).
- S.Y. Wang, X. Wang and S.P. Jiang, *Phys. Chem. Chem. Phys.*, **13**, 6883 (2011).
- C.B. Liu, K. Wang, S.L. Luo, Y.H. Tang and L.Y. Chen, *Small*, **7**, 1203 (2011).
- X.B. Yan, J.T. Chen, J. Yang, Q.J. Xue and P. Miele, *Appl. Mater. Interfaces*, **2**, 2521 (2010).
- J. Lee, K.S. Novoselov and H.S. Shin, *ACS Nano*, **5**, 608 (2011).
- W.J. Zhao, P.H. Tan, J. Liu and A.C. Ferrari, *J. Am. Chem. Soc.*, **133**, 5941 (2011).
- Y. Zhao, Y. E. L. Fan, Y. Qiu and S. Yang, *Electrochim. Acta*, **52**, 5873 (2007).